N91-26008

SUBLIMATION RATES OF CARBON MONOXIDE AND CARBON DIOXIDE FROM COMET NUCLEI AT LARGE DISTANCES FROM THE SUN.

Zdenek Sekanina, Jet Propulsion Laboratory, California Institute of Technology

One of the more attractive among the plausible scenarios for the major emission event recently observed in Comet Halley at a heliocentric distance of 14.3 AU is activation of a source of ejecta driven by an icy substance much more volatile than water. As a prerequisite for the forthcoming detailed analysis of the imaging observations of this event, a simple model is proposed that yields the sublimation rate versus time at any location on the surface of a rotating cometary nucleus for two candidate ices: carbon monoxide and carbon dioxide. The model's variable parameters are the comet's heliocentric distance r and the Sun's instantaneous zenith angle z. Following a technique developed for water ice (Sekanina 1988, *Astron. J.* **95**, pp. 911–924), the sublimation rate $Z(z,r)$ calculated from the equation of energy balance is approximated as follows

$$Z(z,r) = Z_0(r) \cdot \zeta(z,r),$$

where $Z_0(r)$ is the peak sublimation rate at r, which occurs at the subsolar point, and

$$\begin{aligned} \zeta(z,r) &= \cos z - f(r) \cdot \sin^2 z \qquad \text{for } 0 \le z \le z_c, \\ &= 0 \qquad\qquad\qquad\qquad\quad \text{for } z > z_c. \end{aligned}$$

Here $z_c = \arccos\{[1+(2f)^{-2}]^{1/2} - (2f)^{-1}\}$ is the Sun's critical zenith angle, beyond which the sublimation rate is negligible compared with that at the subsolar point. This approximation allows one to write the rotation-averaged sublimation rate $\langle Z \rangle$ at a given r as

$$\langle Z \rangle = (Z_0/\pi) \cdot (a\,\Theta_c + b \sin\Theta_c + c \sin 2\Theta_c),$$

where $\Theta_c(r)$ is a critical hour angle of the Sun that depends upon z_c and the cometocentric latitudes of the active source, $\phi_{\rm act}$, and the subsolar point, $\phi_{\rm ss}$,

$$\cos\Theta_c = \cos z_c \sec\phi_{\rm act} \sec\phi_{\rm ss} - \tan\phi_{\rm act} \tan\phi_{\rm ss},$$

and the coefficients a, b, and c are functions of $\phi_{\rm act}$, $\phi_{\rm ss}$, and $f(r)$. The calculated peak sublimation rate $Z_0(r)$ is for either ice expressed with high precision by

$$\log Z_0(r) = A + B \log(r/r_0) + C\,(r/r_0)^{\beta} + D \log\{1 + (r/r_0)^{\gamma}\},$$

where A, B, C, D, β, and γ are constants for the given ice and r_0 is a "normalizing" heliocentric distance that is related to the ice's sublimation heat L (crudely, $r_0 \propto 1/L^2$). For CO the function $f(r)$ is fitted empirically by

$$f(r) = E\,(r/r_0)^2 \left\{1 + F(r/r_0) + G\,(r/r_0)^2\right\}.$$

For CO_2 this expression yields a fit that is somewhat inferior to that offered by a law

$$f(r) = \tilde{E}\,(r/r_0)^{7/4} \exp\left\{\tilde{F}\,(r/r_0)^{\tilde{G}}\right\}.$$

With r in AU and $Z(r)$ in molecules/cm^2/s, the numerical values of the coefficients are listed in the table below for an assumed unit bolometric emissivity and an albedo of 4 percent. The coefficients A through γ provide an excellent fit up to $r \approx 500$ AU for CO and up to $r \approx 40$ AU for CO_2. The coefficients E through G offer a very good fit up to $r \approx 300$ AU for CO and the coefficients E through $\tilde{G}$ are applicable up to $r \approx 20$ AU for CO_2.

Ice	r_0 (AU)	A	B	C	D	β	γ	E	F	G	$\tilde{E}$	$\tilde{F}$	$\tilde{G}$
CO	285	14.184	−2.00	−0.74	−0.63	2.09	14.95	1.386	−1.337	1.343	...	...	...
CO_2	20.2	15.961	−1.95	−0.75	−1.74	1.50	8.55	1.882	−1.775	1.779	0.78	0.90	2.70

A COMPARATIVE EFFICIENCY OF NUMERICAL ALGORITHMS BASED ON KS-REGULARIZATION OF EQUATIONS OF MOTION OF UNUSUAL MINOR PLANETS AND COMETS; V.A.Shefer, Tomsk State University, Tomsk, USSR

This paper concentrates on application of regularizing and stabilizing KS-transformation in the problem of investigation of the motion of unusual minor planets and comets. The equations of motion of a minor body in KS-variables and the variational equations in heliocentric and planetocentric systems of coordinates are used. A short description of the peculiarities of software realizing developed algorithms is given. The original results of the investigation of efficiency of the algorithms and the application package are discussed on the example of motion of unusual minor planets Icarus and Geographos as well as comets Halley, Honda-Mrkos-Pajdusakova and Gehrels 3.

INTERPRETING ASTEROID PHOTOMETRY AND POLARIMETRY USING A MODEL OF SHADOWING AND COHERENT BACKSCATTERING

Yu. G. Shkuratov † and K. O. Muinonen ‡

† Astronomical Observatory of Kharkov State University,
Sumskaya Street 35, Kharkov 310022, U.S.S.R.
‡ Lowell Observatory,
1400 West Mars Hill Road, Flagstaff, AZ 86001, U.S.A.

Theoretical models of the opposition effect and of negative polarization (or polarization reversal) are usually based on geometric optics. However, such models do not explain some experimental findings; for example, the enhancement of both the opposition effect and negative polarization with decreasing particle size down to wavelength scales.

We have proposed a multiple–scattering interference explanation for these findings (Muinonen 1989, Shkuratov 1988 and 1989) and have outlined two different approaches. One was based on exact electromagnetic solutions for simple scattering systems that include dipole–dipole and dipole–surface coupling; surface–surface coupling was studied in the geometric optics approximation (including phase). The other approach was based on a point–scatterer approximation characterized by model photometric and polarimetric phase functions, and the shadowing effect was derived from the virtual volumes associated with the point–scatterers. Both approaches yielded qualitatively similar results, although neither was entirely satisfactory. We regard them as prototypes for a future unified model of shadowing and coherent backscattering.

Using the aforementioned calculations, two particular results for asteroids can be stated:
(a) The observed opposition effect and negative polarization require the existence of micron–scale fine structure in regolith particles. Although such small–scale structure has been widely assumed in the past, it is not predicted by previous theoretical models.
(b) Recently, a sharp and narrow opposition effect (the so–called opposition spike) has been observed for some bright asteroids. In contrast, weak or non–existent opposition effects are exhibited by some dark asteroids. Such observations are explained by the coherent multiple backscattering mechanism.

References.

Muinonen, K. (1989). Proc. 1989 URSI EM–Theory Symp. (Stockholm), 428–430.
Shkuratov, Yu. G. (1988). Kin. Phys. Neb. Tel **4**, 4, 33–39.
Shkuratov, Yu. G. (1989). Astron. Vestn. **23**, 2, 176–180.

HYDROTHERMAL PROCESSING OF COMETARY VOLATILES

Everett L. Shock and William B. McKinnon
Department of Earth and Planetary Sciences and McDonnell Center for the Space Sciences, Washington University, St. Louis, MO 63130 USA

Cometary volatiles can be processed through hydrothermal systems in several settings in the solar system. Molten cometary ices may circulate through hot rocks during the heating of larger comets, asteroids, or planetesimals caused by decay of radioactive elements or accompanying capture by still larger bodies. If so, the resulting aqueous solutions may be responsible for the aqueous alteration which is documented in carbonaceous meteorites and some interplanetary dust particles. In addition, hydrothermal processes may help explain differences between comets and other volatile-rich outer solar system objects like Triton. It is also possible that cometary volatiles were processed through hydrothermal systems subsequent to their arrival on the early Earth, which may have implications for the origin of life. The chemical consequences of this hydrothermal reprocessing of cometary volatiles can be assessed with speciation and mass transfer calculations which explicitly account for changes in temperature, pressure, and oxidation state. Temperature and pressure profiles can be predicted for various heating mechanisms, and redox conditions can be evaluated from reactions between hydrothermal fluids and various mineral assemblages. For example, subsequent to its capture by Neptune, Triton would have experienced an episode of tidal heating sufficient to melt its icy mantle and possibly its rocky core as well. This heating would have driven hydrothermal circulation at the core-rock/mantle-ocean boundary. By assuming an initial cometary composition for the icy mantle and evaluating the effects of changes in temperature and oxidation state, we find that hydrothermal processing helps to explain the presence of nitrogen and the lack of carbon monoxide in Triton's atmosphere. In addition, depending on the temperature and prevailing oxidation state, ammonia, as well as acetic acid, ethanol, urea, and ethanamine are possible components of Triton's resulting mantle material. A principal uncertainty that needs to be addressed is the range of cometary compositions, particularly with respect to overall carbon and nitrogen relative abundances, and the partitioning of carbon between relatively unreactive methane and other cometary species. Calculations of a similar nature can be used to examine the consequences of reactions between molten cometary ices and possible initial mineral assemblages of chondrite parent bodies. Temperature and compositional constraints imposed by the petrologic and isotopic evidence for aqueous alteration can then be used to test the possibility of organic compound synthesis during the aqueous alteration events.

SYSTEMATIC SURVEY FOR BRIGHT JUPITER TROJANS; C.S. Shoemaker, E.M. Shoemaker, R.F. Wolfe, U.S. Geological Survey, Flagstaff, AZ 86001, and E. Bowell, Lowell Observatory, Flagstaff, AZ 86001

A systematic survey for bright Jupiter Trojans using the Palomar 46-cm Schmidt was initiated in late 1985 [1,2]. Renewed work was begun on the L4 region in 1988, and an intensive examination of the L5 region was made in the fall of that year. The survey has been continued each subsequent year with the goal of finding all Trojans brighter than H=10.25 and of obtaining precise, multiple-opposition orbits for all known bright Trojans. Concurrently, surveys for faint Trojans are being carried out by L.M. French, S.J. Bus, and E. Bowell, using the Cerro Tololo 61-cm Schmidt, and by E. Bowell and K. Russell, using the U.K. 1.2-m Schmidt [3].

To date, 57 Trojans have been found with the 46-cm Schmidt, 30 in the L4 swarm and 27 in L5. In 12 cases, previously known Trojans with short-arc orbits were rediscovered; multiple opposition orbits were thus obtained. Five Trojans found independently at Palomar were discovered nearly simultaneously at other observatories. Eighteen of the Trojans found with the 46-cm Schmidt are now numbered; positions have been measured on multiple oppositions for all but 12 of the remaining objects.

A question of considerable interest has been the relative sizes of the L4 and L5 swarms [4]. Our new discoveries have increased the number of known L5 Tojans brighter than H=10.25 by about 60%. We conclude that discovery probably is now complete to H ≈ 9, the approximate magnitude of the brightest object that we found in 1988. At this magnitude, the cumulative numbers of objects in the L4 and L5 swarms are nearly the same. Although we have found roughly equal numbers of new L4 and L5 Trojans, the mean magnitude of our L4 Trojans is about 0.2 mag brighter than that of our L5's. This difference is the consequence of exceptionally good observing conditions in the fall of 1988. It is clear that L5 Trojans are less numerous than L4's at magnitudes fainter than H = 9.25, but the difference appears to be only about 30%, at least for Trojans brighter than H = 10.25. We suggest that, at fainter magnitudes, the magnitude-frequency distribution of the L5 population is parallel with the distribution estimated for L4 by Shoemaker et al. [1]. This suggested distribution for the L5 population is close to that estimated by van Houten et al. [5] for L4. By extrapolation, we infer that there are about 100 L5 Trojans brighter than H = 11.

The mean inclination of the Trojans found with the 46-cm Schmidt is 17.6 degrees in the L4 swarm and 16.0 degrees in L5. The value for the L5 swarm is slightly less than the mean of 17.7 degrees estimated by Shoemaker et al. [1] for the total Trojan population, probably because of lack of coverage of the L5 libration region at high southern ecliptic latitudes.

The large increase in multiple opposition orbits available for L5 Trojans has led to a successful search of the L5 swarm for dynamical pairs or groups of possible collisional origin. We calculated proper elements by analytical methods presented in [6] for 75 multiple opposition orbits of L5 Trojans. Libration amplitude (D), proper eccentricity (e_p), and proper inclination (i_p) obtained by analytical methods are similar to the proper elements obtained by Bien and Schubart by numerical integration for 21 numbered L5 Trojans [7]. Ten fairly closely matched dynamical pairs and one dynamical group of three Trojans were found. Calculated velocities of separation for the recognized pairs and within the group of three are comparable with separation velocities between members of main asteroid belt families.

References: [1] Shoemaker, E.M., Shoemaker, C.S., and Wolfe, R.F., 1989, in Binzel, R.P., Gehrels, T., and Matthews, M.S., eds., Asteroids II, Tucson, Univ. Ariz. Press, p. 487-524. [2] Shoemaker, C.S., and Shoemaker, E.M., 1988, Lunar and Planet. Sci. 19, p. 1077-1078. [3] French, L.M., Vilas, F., Hartmann, W.K., and Tholen, D.J., 1989, in Binzel, R.P., Gehrels, T., and Matthews, M.S., eds., Asteroids II, Tucson, Univ. Ariz. Press, p. 468-586. [4] Degewij, J., and van Houten, C.J., 1979, in Gehrels, T., ed., Asteroids, Tucson, Univ. Ariz. Press, p. 417-435. [5] van Houten, C.J., van Houten-Groeneveld, I., and Gehrels, T., 1970, Astron. J., v. 75, p. 659-662. [6] Levison, H.F., Shoemaker, E.M., and Wolfe, R.F., 1991, Lunar and Planet. Sci. 22, p. 803-804. [7] Bien, R., and Schubart, J., 1987, Astron. Astrophys., v. 175, p. 292-298.

GEOLOGICAL AND ASTRONOMICAL EVIDENCE FOR COMET IMPACT AND COMET SHOWERS DURING THE LAST 100 MILLION YEARS.
E. M. Shoemaker, U.S. Geological Survey, Flagstaff, AZ 86001.

The present near-Earth flux and magnitude distribution of asteroids and comets can be estimated from discovery rates in systematic surveys of the sky and from the total record of discoveries. These observations have been utilized to calculate the present rate of cratering on Earth by impact of asteroids and comets [1]. The cumulative magnitude-frequency distribution of Earth-crossing asteroids drops steeply, roughly as $\Sigma N \propto e^{2H}$, at magnitudes brighter than about H = 16 [1]. Systematic observations by Roemer, on the other hand, suggest that the distribution of nuclear magnitudes of Earth-crossing comets follows a flatter distribution, approximately of the form $\Sigma N \propto e^{0.9H}$, up to the brightest objects observed [2]. Because of this difference, Shoemaker et al. [1] estimated that asteroid impacts have dominated the production of craters <50 km in diameter over the last 100 Myr, but that comet impacts may have produced most craters >50 km in diameter. The largest known impacts, therefore, are the ones most likely to yield evidence of the collision of comets.

The impact event at the K/T boundary probably was the most energetic of the past 100 Myr. An impactor with a diameter of order 10 km has been suggested from the observed column abundance of siderophile elements at the boundary [3]. This size body would produce a crater about 150 km in diameter [4, 5]; if the object were a comet, the diameters of the projectile and the crater might have been somewhat greater. The abundance pattern of the siderophile elements at the boundary appears to be consistent with a primitive body. Three structures of known or possible impact origin may be associated with the boundary event: 1) the 35-km-diameter Manson structure in Iowa [6], 2) the ~100-km-diameter Popigai structure in Siberia [7], and 3) the ~180-km-diameter Chicxulub structure in Yucatan [8, 9]. The Popigai structure is the largest firmly identified Phanerozoic impact crater; Chicxulub, if confirmed as an impact crater, would be one of the largest known impact structures on Earth. If these structures are similar but not identical in age, they might have been formed by a comet shower. On the other hand, two impact events appear to be represented by two successive thin clay layers at the K/T boundary in western North America. Because the two clay layers are in contact, wherever they have been recognized, the two impact events must have been very closely spaced in time. The distribution and lithology of shocked grains in the upper clay layer suggest that the Manson structure is a likely source of these grains [10]. Stratigraphic relationships in the Gulf of Mexico-Caribbean region point strongly to a large crater in that region [11, 12]. Chicxulub is a likely source of the K/T boundary deposits in the surrounding region and also of the lower clay layer in western North America. Manson and Chicxulub may have been produced by fragments of a single very large comet that had been disrupted to form a compact comet stream, perhaps analogous to the present group of sun-grazing comets.

At least three separate large impact events fairly closely spaced in time were associated with a step-wise mass extinction in the late Eocene. These impacts are recorded in deep-sea sediments by two horizons of impact-glass spherules in the *Globorotalia cerroazulensis* foraminiferal zone and by a third spherule horizon in the underlying *Globigerapsis semiinvoluta* zone [13]. An Ir anomaly coincides with the lower spherule horizon of the *G. cerroazulensis* zone; an Ir anomaly recognized in the *G. semiinvoluta* zone in Italy probably is correlative with the *semiinvoluta* spherule horizon [14]. No craters related to the spherule horizons have yet been identified, although two craters of similar age are known. The time interval separating the deposition of the lowest and highest spherule horizons is about 1 to 2 Myr, consistent with the theoretical duration of a comet shower [15]. The upper two spherule horizons are separated by about 30 cm stratigraphically and probably by less than 100,000 years in time. It is unlikely that the close spacing in time of the three spherule-producing impacts and their association with extinction steps are due to chance [16]. The late Eocene extinction steps are coincident with episodes of cooling of the oceans, and the end of the Eocene is marked by abrupt cooling of the oceans [17] and by major glaciation in Antarctica. A mild comet shower evidently occurred in the late Eocene, and it appears to have triggered a shift in global climate.

The present flux of long-period comets may also correspond to a mild comet shower. If the flux of comets at the present level is extrapolated back over time, the estimated production of large craters by comet impact is about equal to the observed record on the Moon of large craters younger than 1.0 Gyr. But the lunar crater record must reflect comet showers as well as the background rate of comet impact. Hence the present comet flux is estimated to be not less than twice the background flux [1]. Furthermore, several surges in the flux of large Earth-crossing asteroids probably occurred during the last 1.0 Gyr, owing to catastrophic breakup of large bodies in the main asteroid belt [18]. If so, most large craters on the Moon younger than 1.0 Gyr are more likely to have been formed by impacts of asteroids than of comets. The present comet flux, in this case, must be several times higher than the mean flux over the last 1.0 Gyr (including the contribution from showers). Onset of the inferred present comet shower might be correlated with the beginning of strong advances of northern hemisphere continental icecaps in the Pleistocene. The great strewn field of Australasian tektites and microtektites may be a signature of one or more large comet impacts during this shower.

References: [1] Shoemaker, E.M., Shoemaker, C.S., and Wolfe, R.F., 1990, Geol. Soc. Amer. Spec. Paper 247, 155-170. [2] Shoemaker, E.M., and Wolfe, R.F., 1982, in Morrison, D., ed., The Satellites of Jupiter, Tucson, Univ. Arizona Press, 277-339. [3] Alvarez, L.W., et al., 1980, Science, 208, 1095-1108. [4] Emiliani, C., Kraus, E.B., and Shoemaker, E.M., 1981, Earth and Planet. Sci. Lett., 55, 317-334. [5] Roddy, D.J., et al., 1987, Internat. Jour. of Impact Engineering, 5, 525-541. [6] Kunk et al., 1989, Science, 244, 1565-1568. [7] Deino, A.L., Garvin, J.B., and Montanari, A., 1991, Lunar and Planet. Sci. Conf. XXII, 297-298. [8] Hildebrand, A.R., and Penfield, G.T.,1990, EOS, 71, 1425. [9] Kring, D.A., Hildebrand, A.R., and Boynton, W.V., 1991, Lunar and Planet. Sci. Conf. XXII, 755-756. [10] Izett, G.A., 1990, Geol. Soc. America Spec. Paper 249. [11] Hildebrand, A.R. and Boynton, W.V., 1990, Science, 248, 843-846. [12] Alvarez, W., et al., 1991, Lunar and Planet. Sci. Conf. XXII, 17-18. [13] Keller, et al., 1987, Meteoritics, 22, 25-60. [14] Montanari, A., 1990, EOS, 71, 1425. [15] Hut, et al., 1987, Nature, 329, 118-126. [16] Shoemaker, E.M., and Wolfe, R.F., 1986, in Smoluchowski, R., Bahcall, J.N., and Matthews, M., eds., The Galaxy and the Solar System, Tucson, Univ. Ariz. Press, 338-386. [17] Kennett, J.P., and Shackleton, N.J., 1976, Nature, 260, 513-515. [18] Shoemaker, E.M., 1984, in Holland, H.D., and Trendall, A.F., eds., Patterns of Change in Earth Evolution, Dahlem Konferenzen F.R.G., Springer-Verlag, 15-40.

ON THE DISTRIBUTION OF MINOR PLANET INCLINATIONS; V. A. Shor, Institute of Theoretical Astronomy, USSR Academy of Sciences, E. I. Yagudina, Institute of Applied Astronomy, USSR Academy of Sciences

The distributions of the asteroid orbits with inclination and the longitude of ascending node on the ecliptic plane have been studied. The position of the plane that can be considered as the mean plane of the asteroid belt has been determined. The distribution of inclinations of the asteroids with respect to this plane has been constructed and its distinctive features are discussed.

RECOVERY OF THE AVERAGED MODEL OF COMETARY GRAIN BY POLARIMETRIC DATA;
L.M.Shulman, The Main Astronomical Observatory of the Ukrainian Academy of Sciences, 252127, Kiev, USSR

The standard approach to interpretation of cometary polarimetric data is the numerical solution of a set of direct light scattering problems with the variation of parameters and subsequent comparison of the results with the observational data. One needs to take the definite shape, refraction index and the distribution of the grains on size in order to calculate the picture of the scattering of light.

The classic Mie's theory is not valid for irregular (shapeless or non-uniform) particles. In such cases the couple dipole method [1] was recently used to calculate the scattering by fluffy particles. Another approach to analyses of observational data is proposed here. It is based on the solution of the inverse problem of light scattering. No parameters of the dust particles should be presetted before the calculation. The input information for the analyses is the observed spacial distribution of the Stokes parameters [2]. Therefore, using appropriate hypothesis on symmetry and asymptotic behaviour of the Stokes parameters one can obtain the averaged size and shape of the comet dust particle as well as the distribution of refractivity inside it.

REFERENCES

1. Gustafson, B.A.S., Zerull, R.H., Corbach, E., and Schulz, K. in: Fluffy structures. II., ed. by P.M.M. Jenniskens and J.I.Hage, Leiden, 1989, P. 3-6.
2. Shulman, L.M., Comet Circular N. 414, Kiev, 1990, P. 7-8.

DIURNAL VARIATION OF OVERDENSE METEOR ECHO DURATION AND OZONE; Miloš Šimek, Astronomical Institute of the Czechoslovak Academy of Sciences, Ondřejov, Czechoslovakia.

Diurnal variation of median duration of overdense sporadic radar meteor echoes is examined. The meteors recorded in December, January and August by Ondřejov meteor radar for a period 1958-1990 have been used for the analysis. Maximum median echo duration located 1-3 hours after local sunrise at meteor height confirms already known sunrise effect. Minimum echo duration occuring at sunset-time seems to be an effectual point of diurnal variation of the echo duration, when ozone is no more dissociated by solar UV radiation. The effect of diurnal change of echo duration should be considered when mass-distribution of meteor showers is analysed.

Melting, Vaporization, and Energy Partitioning for Impacts on Asteroidal and Planetary Objects: Catherine L. Smither and Thomas J. Ahrens, Lindhurst Laboratory of Experimental Geophysics, Seismological Laboratory, California Institute of Technology, Pasadena CA 91125

Our study focuses on the effects of impacts of silicate projectiles on asteroidal and planetary-sized silicate targets, simulating these impacts using a 3-D Smoothed Particle Hydrodynamics (SPH) code [1,2]. Three target sizes are considered here: radii of 6400, 1700, and 100 km. For the two larger cases, the impactor velocity was varied from 10 to 20 km/sec, and the impactor was 60% of the radius of the 6400 km target, and 40% of the 1700 km target. For the smallest bodies, impactor and target were the same size. Both normal and oblique (60° offset between the centers of the target and impactor bodies) were modeled.

In the simulation of the larger bodies, the entire impactor was shocked to internal energies sufficient for complete melting. In addition, as much as 38% of the target (3.5 projectile masses) was melted in the case of a normal impact at 20 km/sec on the 6400 km radius target. Lower impact velocities produced less melt in the target; an impact at 10 km/sec on the 1700 km radius target melted only 15% or .5 projectile masses of the target material. The 10 km/sec impacts were not sufficient to vaporize more than 25% of the impactor and 1% of the target mass. Higher velocity impacts vaporized 6% of the target and 82% of the impacts in the case of a normal impact on the 6400 km body. Models of the 100 km impacts at 5 km/sec show a total of 1.4 projectile masses melted, of which 0.35 projectile masses vaporized. The effects of impact-induced rotation and the balance between accretion, co-orbiting ejecta and erosion versus impact velocity and encounter orientation will also be addressed.

Initially, the bulk of the energy in the system is in the kinetic energy of the impactor. After impact, this energy is partitioned into the kinetic and internal energies of the target and the impactor. Studies of impacts on a half-space [3] predict that little or none of the initial energy will remain in the kinetic energy of the impactor after the first stages of impact. The results of these simulations, however, show that the kinetic energy of the impactor particles can remain a significant amount of the initial energy of the system. The figure below show the energy budget for two simulations of impacts at 10 km/sec on the 1700 km radius planet. The energy is normalized to the initial energy; time is plotted as dimensionless time τ=Ut/a, where U is the impact velocity, t is the time after impact, and a is the radius of the impactor. The amount of the total energy remaining the the kinetic energy of the impactor is much greater in the case of a normal impact than for an oblique impact, since more of the impactor travels at a higher velocity away from the target. The same plot for the 20 km/sec impact shows a greater proportion of the total energy in the kinetic energies of both bodies. For the largest targets, the final internal energy as a percent of the total energy is higher than in the case of the 1700 km impacts; 38% as opposed to 29% for the targets in the 20 km/sec normal impacts and 41% vs 18% for the oblique 10 km/sec impacts.

References:

[1] Monaghan JJ and Gingold RA (1983) *J. Comput. Phys.*52 374-389.

[2] Benz W, Slattery, WL amd Cameron AGW (1986) *Icarus* 66 515-535.

[3] O'Keefe JD and Ahrens TJ (1977) *Proc. Lunar Sci Conf 8th*, 3357-3374.

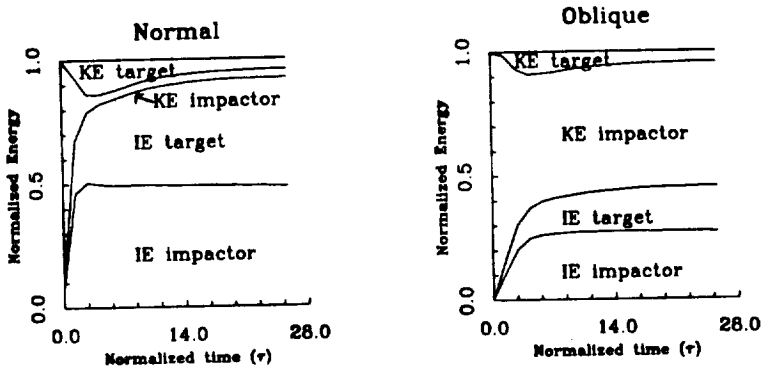

Impact budget for normal and oblique impacts on a 1700 km target at 10 km/sec.

PRELIMINARY ORBITS OF TROJAN ASTEROIDS; A.G.Sokolsky, Institute of Theoretical Astronomy of USSR Academy of Sciences

There are many attempts to construct the semi-analytical theories of Trojan asteroids which are based on the assumption of their proximity to the triangular libration points of Sun-Jupiter system within the framework of the restricted three-body problem. But as it was shown by Yu.Riabov [1] it is not possible to construct a Trojan theory with sufficient precision if the libration point itself is taken as the first approximation orbit. For this reason the idea to select preliminary orbit from other particular solutions of the three-body problem looks quite natural.

It is possible to take as such approximation the finite amplitude periodic orbit which is numerical extending (with respect to the constant of energy) small periodic motions in the vicinity of the triangular libration points of the three-body problem. The predictor-corrector method in the Hamiltonian modification [2] (about Lagrangian modification see [3]) was used for construction of the periodic orbits family. The concrete values of parameters which separate the preliminary orbit of each Trojan from three-body problem periodic solutions can be found as the result of processing of many year observations by least square method.

The preliminary orbit may be improved in future by KAM-theory taking into account the eccentricity of Jupiter orbit, Saturn gravitational action and other perturbation effects.

1. Riabov Yu.A. On the periodic solutions in the vicinity of the triangular libration points of plane restricted three-body problem.- Soviet Astron.J., 1952, v.29, N 5, pp.582-596.

2. Karimov S.R., Sokolsky A.G. A method of extending (with respect to the parameters) the natural families of periodic motions of Hamiltonian systems. - Preprint ITA Acad.Sci.USSR, 1990, N 9.

3. Karimov S.R., Sokolsky A.G. Periodic motions, generated by Lagrangian solutions of the circular restricted three-body problem. - Celestial Mechanics, 1989, v.46, N 4, pp.335-381.

ORBITAL EVOLUTION OF OUTER BELT ASTEROIDS IN SPACE CASE;
N.A.Solovaya, and I.A.Gerasimov, Celestial Mechanics Department, Sternberg State Astronomical Institute, 119 899 Moscow, U.S.S.R.

The evolution of minor planets of the outer part of the asteroidal belt for different inclinations of their orbits is investigated. It is considered in the framework of the semi-averaged elliptic restricted three body problem. The Jacobi's integral exists. Regions of the Hill's stability and unstability are defined. Numerical investigations showed that the regions of the stability are becoming smaller for increasing orbital inclinations. Some asteroids of the Hilda group can be in the unstable region, but their orbits are librators.

THE TAPANUI REGION OF NEW ZEALAND : A "TUNGUSKA" OF 800 YEARS AGO?

Duncan Steel, *Anglo-Australian Observatory, Private Bag, Coonabarabran, NSW 2357, Australia;* and
Peter Snow, *Suffolk Street, Tapanui, Otago, New Zealand.*

Near the town of Tapanui in the province of Otago in the south of New Zealand is a structure known as the Landslip Crater. Although there is some doubt that this is a scar formed by an impact upon the Earth's surface of a large solid body, there is much evidence that links this site to a major cataclysm around 800 years ago. The area apparently contains many peculiar gelogical features, and it has been claimed that the "images" of plants and avian materials on rock surfaces may have been formed by an intense high-temperature flash, like an ash glaze in pottery. There is much physical evidence for a widespread fire at about that time, possibly followed by a deluge, and this has usually been ascribed to the indigenous Maoris using fire to drive the now-extinct Moas (*Dinornis*: a giant terrestrial bird) from the forests. However, studies of tree falls and their distribution indicate a rather more coherent event. There is also the evidence of Maori myth, legend, poetry and song which speak of the falling of the skies, raging winds, upheaval of the Earth, and mysterious devastating fires from space. Many local place names may be translated in terms of a catastrophic event having occurred thereabouts, and Tapanui itself apparently means "The Big Explosion". One Maori lament states that:

> "Very calm and placid have become the raging billows,
> That caused the total destruction of the Moa,
> When the horns of the Moon fell from above down."

The purpose of this paper is to bring the site to the attention of scientists with expertise in the various areas which would be necessary for a rigorous study of the area, in order to show whether or not a Tunguska-type event did occur there around the twelfth century.

1991 DA : AN ASTEROID IN A BIZARRE ORBIT

Duncan Steel and Rob McNaught,
Anglo-Australian Observatory,
Private Bag, Coonabarabran, NSW 2357, Australia

David Asher,
Department of Physics, University of Oxford,
Keble Road, Oxford, OX1 3RH, England, U.K.

Asteroidal object 1991 DA was discovered by R.H.McNaught on a U.K. Schmidt Telescope plate taken on 1991 February 18 by P.McKenzie. Initial solutions were based on an Apollo-type motion (*IAU Circular 5193*) due to the asteroidal appearance of the object, but later observations have shown that it is on one of the most bizarre orbits known for any asteroid: at 61.9 degrees its inclination is the third highest of all known minor planets, and its eccentricity of 0.866 is also the third highest amongst asteroids. With a perihelion distance of 1.58 AU and aphelion at 22 AU, 1991 DA crosses the paths of Mars, Jupiter, Saturn and Uranus, and therefore must have a dynamical lifetime measured in units of only $\sim 10^5$ years. The two other "asteroids" which cross any of the giant planets apart from Jupiter (944 Hidalgo and 2060 Chiron) have much lower eccentricities and have long been suspected as being dormant comets; the detection of comet-like activity in Chiron beginning in 1989 (Hartmann *et al.*, *Icarus*, **83**, 1-15, 1990; Luu & Jewitt, *Astron. J.*, **100**, 913-932, 1990) has confirmed that this belief is well-founded. CCD imaging by English and Freeman (*IAU Circ. 5199*) and by West and by Ryder (*IAU Circ. 5208*) has shown no evidence of a coma despite the fact that 1991 DA is close to perihelion at this time, and spectral observations by Steel and McNaught with the Anglo-Australian Telescope have also shown no evidence of comet-like emissions: thus 1991 DA appears to be an inert asteroid. With regard to the past and future orbit of this body, it is clear that statistical-type numerical integrations like those of Hahn and Bailey for Chiron (*Nature*, **348**, 132-136, 1990) are to be recommended since these may elucidate the path by which the present orbit of 1991 DA has come about. One of us (D.A.) has performed preliminary integrations that show the perihelion distance to have changed from 1.3 AU 10 kyr ago through 1.6 AU at present to 1.8 AU 10 kyr in the future. Over this period the semi-major axis varies non-monotonically between 11.7 and 12.1 AU, the eccentricity drops from 0.89 to 0.85, and the inclination from 72 to 54 degrees. Longer-term integrations indicate that q was less than 1 AU about 20 kyr yr ago. The elements do not appear to be chaotic during ± 25 kyr integrations.

WATER MASERS, RED GIANTS, AND OORT CLOUDS AROUND OTHER STARS; S. Alan Stern (CASA/University of Colorado) and J. Michael Shull (CASA/University of Colorado).

In some 4-5$\times 10^9$ yrs the Sun will exhaust its hydrogen supply and begin its post main sequence evolution. This process is a common one for lower main sequence stars. During their luminous, post main sequence phase, solar-type stars typically attain luminosities of $6 \times 10^3 L_\odot$ for one-to-several hundred million years. The effects of such a luminosity increase on the Sun's comet reservoir will be dramatic. If comet clouds are common around solar-type stars, then prodigious cometary destruction should be a hallmark of post main sequence stellar evolution.

We suggest that destruction of orbiting comets and debris provides a natural mechanism to explain several attributes of giant star outflows. These include:

- The ubiquitous presence of H_2O and OH around post main sequence stars (Jones, et al. 1983; Bowers and Hagen 1984).
- Toroidal OH Outflow Geometries Observed in VLBI Experiments (Bowers, et al. 1989).
- The coexistence of both water-ice and water-vapor at distances of several hundred AU (Jura and Morris 1985). And
- Reports of dust (Stencel, et al. 1989) and complex organics (Geballe, et al. 1989) located at the water condensation radius of many M giants and supergiants.

The competing explanation for water emission around these stars is photochemistry in the stellar outflow (Goldreich and Scoville 1976).

We stress that our models of comet cloud destruction do not indicate that the bulk stellar mass loss itself, nor the high dust mass loss rates common to giant and supergiant stars are the result of comet cloud destruction. However, the source of water in these outflows is easily, and naturally explained by the destruction of orbiting, volatile rich bodies. If confirmed by observations, our work would imply the nearly-ubiquitous presence of comet clouds around other stars. We are untertaking such an observation program as a part of the NASA Origins of Solar Systems Program.

MEASUREMENT CONSTRAINTS ON NOBLE GASES IN A COMET: FAR-ULTRAVIOLET SPECTRA OF COMET AUSTIN (1988c1).

S.A. Stern, J.C. Green, W. Cash, and T.A. Cook (CASA/University of Colorado).

We employ a long-slit spectrum of comet Austin (1988c1) obtained during a 258 second observation by the University of Colorado imaging FUV rocket telescope/spectrometer on 28.4 April 1990 UT to derive meaningful upper limits on the abundance of Ar and He in comet Austin. This far-UV spectrum spans the wavelength range 910-1180 Å, with a resolution of 3 Å. The instrumental effective area is essentially flat across the bandpass, with a value of ~ 0.5 cm^2 in first order.

Comet Austin was a bright comet likely making its first apparition from the Oort Cloud at the time of our observation. The absence of both the 1048 and 1066 Å fluorescence emissions in comet Austin on the date of our observations allow us to place constraints on the formation temperature and subsequent thermal history of this comet. We will discuss the data set, describe how upper limits on Ar I (1048 and 1066 Å observed in first order) and He I (584 Å observed in second order) were obtained, compare these upper limits to an IUE-derived H_2O production rate in 1988c1 extrapolated to our observation date, and then discuss the implications of these results for the origin of comets in general, and comet Austin in particular.

These results constitute the first meaningful spectroscopic upper limits on noble gases in a cometary coma. They also demonstrate the important potential for FUSE satellite FUV spectroscopy of comets in the late 1990s.

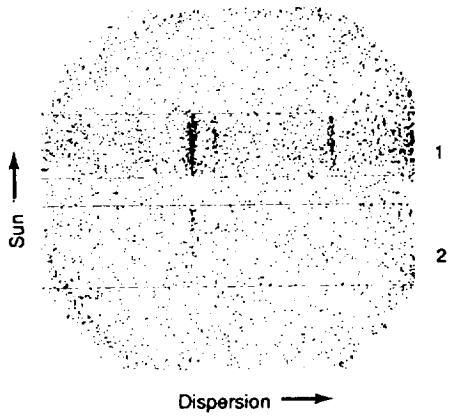

Fig. 1. A plot of all the events recorded during the observation of comet Austin. The numbers 1 and 2 indicate the locations of the primary and secondary slits, respectively. Wavelength increases toward the right. The brightest feature in the primary slit is the feature at 1026 Å. The higher level of background at the extreme right of the detector is due to scattered Lyman α.

CARTOGRAPHY OF ASTEROIDS AND COMET NUCLEI FROM LOW RESOLUTION DATA; Philip J. Stooke, Department of Geography, University of Western Ontario, London, Ontario, Canada N6A 5C2 (Stooke@vaxr.sscl.uwo.ca).

High resolution images of non-spherical objects, anticipated from Galileo, CRAF and Cassini and existing for Phobos and Deimos, lend themselves to conventional planetary cartographic procedures: control network analysis, stereophotogrammetry, image mosaicking in 2D or 3D and airbrush mapping (1). There remains the problem of a suitable map projection for bodies which are extremely elongated or irregular in shape. Where the available data are of very low resolution, as may be expected from speckle interferometry, Hubble Space Telescope images (even after its optics are modified), ground-based radar imaging, convex hull estimates, lightcurve modelling and distant spacecraft encounters, conventional methods of shape determination will be less useful or will fail altogether. This will leave limb and terminator topography as the principal sources of topographic information.

I have developed a method for shape determination based on limb and terminator topography. After initial development (2) and testing (3,4,5) it has been applied to the nucleus of Comet Halley (6) and the jovian satellite Amalthea. The Halley map will be repeated if a new concensus is reached on the rotation state. The Amalthea results, presented here, demonstrate the method itself and the range of cartographic products now available for such bodies.

Voyager images of Amalthea were decompressed from PDS CD-ROMs. Outlines were digitized from enlarged displays, and coordinates converted from display line and sample values to kilometres in the image plane. An initial triaxial ellipsoid model was registered with the digitized outlines and iteratively modified by locally increasing or decreasing radii until the model successfully duplicated all limbs and terminators in the eight images used for modelling. Topography of major craters and ridges was estimated but is very poorly constrained by the data. The model is illustrated with graticules depicting Voyager images (Figure 1), views from mutually perpendicular directions including the polar view not seen by Voyager (Figure 2), and as a Morphographic Conformal Projection (the non-spherical equivalent of the familiar Stereographic) graticule (Figure 3). These can be used as bases for shaded relief, albedo and geological maps of the body. Finally, contour maps of radii and elevations relative to a 280 by 150 by 140 km triaxial ellipsoid are given in cylindrical projections (Figure 4).

The origin of the planetocentric coordinate system is the assumed centre of mass, tested by comparing volumes on either side of three mutually perpendicular planes during modelling. The centre of mass is probably within about 5 km of the position assumed here, assuming uniform or radially symmetrical internal mass distribution. The model is found to have a volume of 2.5 $\pm$ 0.5 million cubic km. Radii are typically uncertain by about 2 pixels (10 to 20 km) near limbs and terminators (less where several intersect), but are very poorly constrained in regions where no limb or terminator traces occur in Voyager coverage. Although limbs can be located to within a pixel on most Voyager images, their geographic locations on the model are uncertain by many degrees, or even tens of degrees in some cases, resulting in lower reliability in the model.

The shape-modelling methods described here may be applied to any object for which low resolution data sets are acquired. The Morphographic map projections are suitable for all non-spherical bodies including those whose shapes are determined by more precise means. Particularly significant uses include registering data obtained from different instruments (e.g. HST images and a radar convex hull) or at different oppositions, and estimating local slopes for photometric studies. The results can be portrayed graphically as shown here, giving base maps for geological interpretation and aids to visualization of the object itself.

REFERENCES: **(1)** Greeley, R. and R.M. Batson, eds, 1990: **Planetary Mapping**, Cambridge University Press. **(2)** Stooke, P.J., 1986: **Proc. 2nd Internat. Symp. Spatial Data Handling**, pp. 523-536. **(3)** Stooke, P.J., 1988: Ph.D. Diss., Univ. of Victoria. **(4)** Stooke, P.J. and C.P. Keller, 1987: **Lunar Planet. Sci. XVIII**, pp. 956-957. **(5)** Stooke, P.J. and C.P. Keller, 1990: **Cartographica** 27 (2): 82-100. **(6)** Stooke, P.J. and A. Abergel, 1991: **Astron. Astrophys.** (in press).

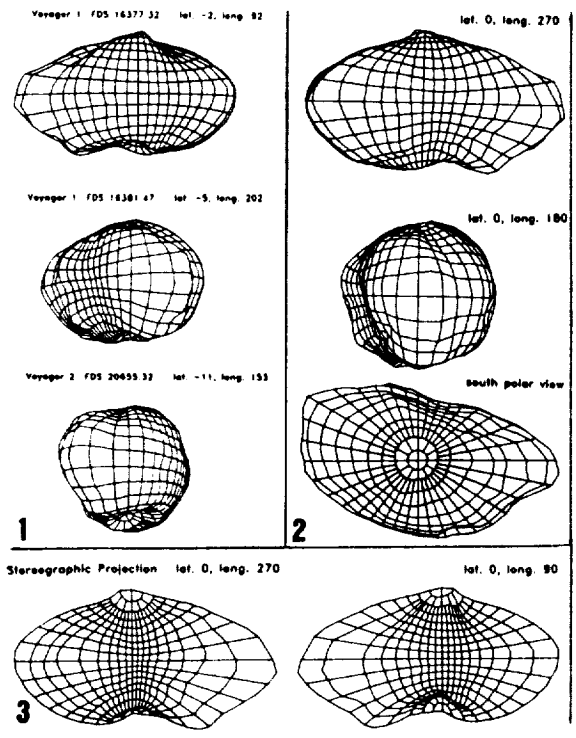

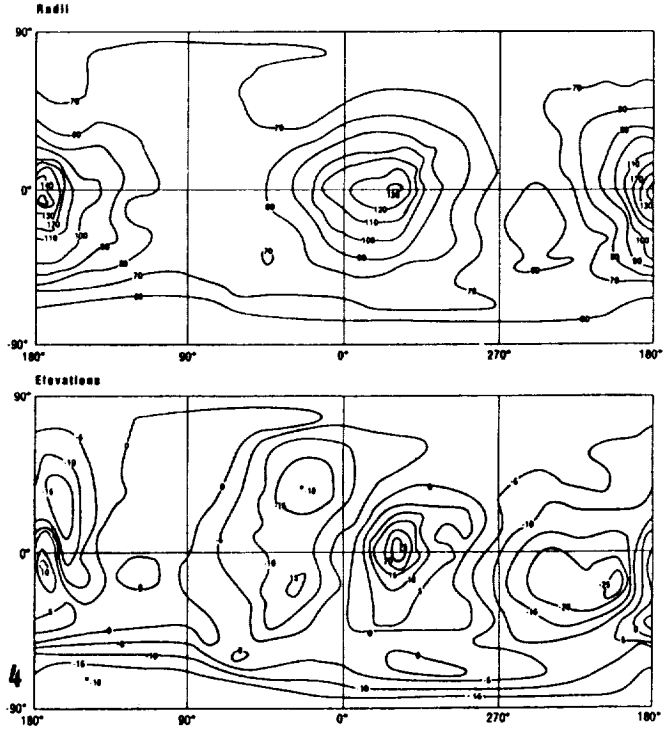

SPECTROPHOTOMETERY OF THE CONTINUUM IN 18 COMETS; A. D. Storrs, A. L. Cochran, and E. S. Barker, Univ. of Texas, McDonald Observatory

We have studied the continuum emission in spectra of 18 comets. We find that the gas-to-dust ratio increases with increasing activity (as measured by the production rate of CN). Approximately equal numbers of comets show changes in continuum brightness with distance from the optocenter equal to, or significantly slower than the canonical $(\text{distance})^{-1}$ falloff. All continuua were red compared to the solar spectrum, with an average reddening of 27 % per 1000 Å. There is some evidence for a change in the slope of the continuum with distance from the optocenter, in some comets. We will discuss trends throughout each comet's apparition as well as comparisons between comets.

C_2 JET IN RECENT COMETS

Bunji SUZUKI*1, Hiroshi KURIHARA*2, and Jun-ichi WATANABE*3
*1 Koshigaya Senior High School, 2788-1,Koshigaya,Koshigaya-shi, Saitama 343 Japan
*2 Kanagawa Industrial High School, 19,Hirakawa-chou Kanagawa-ku, Yokohama 221 Japan
*3 National Astronomical Observatory, Mitaka, Tokyo 181, Japan

We carried out CCD imaging observations of recent three comets (Comet P/Brorsen-Metcalf 1989o, Comet Austin 1989c1 and Comet Levy 1990c). Some jet structures were found out in C_2 images of Comet P/Brorsen-Metcalf and Comet Austin by applying a ring masking technique. The width of these jet structures is at least 45° or more, which is wider than C_2 jets detected in Comet P/Halley(Cosmovici et al. 1988, Clairemidi et al. 1990). The distinctive feature of the C_2 component in Comet Austin is a straight structure extending in the anti solar direction (Fig. 1). This structure reminds us two possible interpretations. One is an edge-on view of a C_2 spiral jet. The other interpretation is a "C_2 tail", which may be caused by the evaporation of the blown-off CHON grains in the invisible CHON tail(Suzuki et al. 1990).

On the other hand, we could not detect any asymmetry in the C_2 images of Comet Levy. The heliocentric distance of this comet during our observation was 1.4 AU which is larger than those of former two comets. This indicates that the production rate of the C_2 molecules in the jet structure depends on the heliocentric distance.

This paper will focus on some results of our C_2 imaging observations, and on discussions of the formation mechanism of C_2 jet structure.

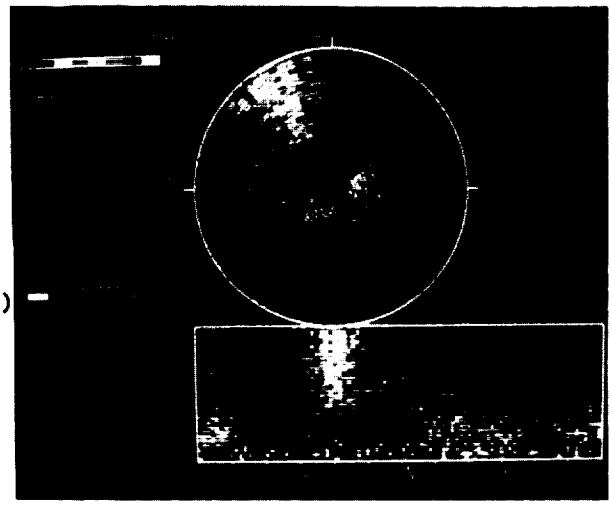

Figure 1
C_2 jets of Comet Austin

Date : 30 Apr. 1990
Time : 18:42:30
Exp. : 240 sec.
Telescope : 60-cm Reflector(f/4.7)

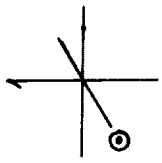

References

Clairemidi,J.,Moreels,G.,and Krasnopolsky,V.A.1990,Icarus,86,115
Cosmovici,C.B.,Schwarz,G.,Ip,W.H.and Mack,P.1988,Nature,332,705
Suzuki,B.,Kurihara,H.,and Watanabe,J.1990,Publ.Astron.Soc.Japan,42,L93

MODELS OF THE FLUX AND ORBITAL DISTRIBUTION OF METEOROIDS

N.T. Svetashkova. Tomsk State University, Tomsk, USSR

The computation method of distribution of flux density and orbital elements from observations of radiometeors rates described in [1] is used. Due to lesser selectivity it gives more exact results than observations of individual orbits of meteoroids, but uncertainty for the antapex area remains. By varying initial conditions and using the results for prognostication of meteor activity we have constructed three models of spatial distribution of meteoroids with masses greater 10^{-4}g , each of which describes observed rates of radio meteors rather precisely. It is shown that in various models heliocentric density of meteoroids for elongation angles from the apex of the Earth's motion $E>160^{\circ}$ at latitudes $|\beta|<20^{\circ}$ can change 20 times remaining practically constant for the other participant of the selestial sphere. Here the number of orbits increases approximately twice with a=1.6-2 AU, $i<20^{\circ}$,q'=2.5-3 AU. Distributions of elements of orbits agree with the results of other authors if they were also obtained from twenty-four-hour observations and cover the whole sky. According to our data the main part of meteoroids move along comet orbits (e>0.7), there is also an increase of their number with e=0.4-0.5, which is characteristic of asteroids of Apollo and Amor groups. The retrograde orbits make up from 5 to 17% in different models, which agrees with inclination orbits of comets, asteroids, bolides and particles of the zodiacal light. However, in contrast to enumerated object there is a considerably isotropic component with arbitrary inclinations $i>30^{\circ}$(~50%). The distribution of perihelion distances shows that about half of the orbits have q'>5 AU, but there is also a maximum of the order 20% in the region q'=2.5-3 AU.

[1] Svetasnkova, N.T. and Sukhotin, A.A. 1990.IN Asteroids, Comets, Meteors III, Uppsala, 575.

METEORITE EVIDENCE FOR NOBLE GASES IN ANCIENT ASTEROIDAL ATMOSPHERES;
Timothy D. Swindle, Lunar and Planetary Laboratory, University of Arizona, Tucson AZ 85721

Asteroids are typically described as "atmosphereless" bodies. However, such a description is only relative. Although they clearly lack the thick, permanent atmospheres of planets like Earth, Moon and Mars, or even the dramatic temporary atmospheres of comets, there will be gas molecules in the vicinity of asteroids, and hence, like the Moon and Mercury (1), there will be atmospheric processes of some sort occurring, starting with neutral atoms in ballistic trajectories. In fact, asteroidal atmospheric processes may provide a method for determining when meteorite regolith breccias were exposed to the solar wind, a parameter that is currently largely unconstrained, although published assumptions range from 4.55 Ga ago (2) to just before ejection into an Earth-crossing orbit (3).

The primary loss mechanism for noble gases heavier than He in the lunar atmosphere is not Jeans escape, but photo-ionization by solar ultraviolet radiation followed by acceleration by the electromagnetic fields associated with the solar wind. Some of the ionization occurs at locations where the ion will be accelerated toward the lunar surface, so some atoms should be implanted (along with the impinging solar wind) into surficial grains. This effect is apparently observed for K-derived ^{40}Ar (4) and probably observed for I- and Pu-derived Xe (5), since variable amounts of the decay-produced noble gases are found intimately associated with solar wind. Since the rates at which these species are produced within the moon decrease with time as a result of decay, the ratio of implanted decay products to implanted solar wind may depend on the time of exposure (5,6).

A similar Xe effect has recently been observed in two gas-rich meteorites, although there is no evidence for any Ar effect (7). Since the two meteorites were both howardites, believed to be samples of the regolith of Vesta or a Vesta-like asteroid, it is important to consider whether a Vestal atmosphere could produce the effect believed to be responsible on the moon.

Calculations based on simplified analytical models (8) suggest that the lifetime against Jeans escape for Xe on Vesta is about an order of magnitude longer than for Ar. Furthermore, the threshhold for photoionization occurs at a longer wavelength for Xe than for Ar, and Xe photoionization cross-sections are higher (9), so a Xe effect is more likely than one for Ar. The details of how much Xe could be implanted depend sensitively on several factors, including the asteroid's size (which determines escape velocity), location (which determines temperature, and hence thermal velocity), and outgassing efficiency; the time of exposure (little decay-produced Xe should have been available more recently than 4 Ga ago); the exact photoionization cross-section rate (which depends on asteroid location, solar UV flux and solar UV spectrum); and the details of the interaction of a neutral Xe atom with the surface (in particular, how quickly it is thermalized). These factors have all been considered in more or less detail (e.g., by adjusting the input parameters in a Monte Carlo model), and the results suggest that photoionization and implantation of decay-produced noble gases might indeed be observable.

References: (1) Hunten et al. (1988) Mercury (U. Arizona), p. 562; (2) e.g., Caffee et al. (1987) Astrophys. J. 313, L31; (3) e.g., Housen et al. (1979) Icarus **39**, 317; (4) Manka and Michel (1970) Science **169**, 278; (5) Swindle et al. (1985) Origin of the Moon (LPI), p. 331; (6) e.g., Eugster et al. (1983) Lunar Planet. Sci. XIV, 177; (7) Swindle et al. (1990) Geochim. Cosmochim. Acta **54**, 2183; (8) Spitzer (1952) Atmospheres of the Earth and Planets (U. Chicago), p. 211; (9) Samson (1982) Handbuch der Physik **31**, 123.

DUST TRAILS AND THE NATURE OF COMETS; M. V. Sykes, University of Arizona, and R. G. Walker, Jamieson Science and Engineering

Cometary dust trails were first observed by the Infrared Astronomical Satellite and consist of large refractory particles ejected from short-period comets at low velocities. Comets observed to have trails by IRAS tend to lose the bulk of their mass in the large refractory trail particles, and are found to have a median refractory/volatile mass ratio of ~ 3. An examination of IRAS observation selection effects in a survey of dust trails indicates that trails are common to all short-period comets. We suggest that comets in general may be more like "frozen mudballs" than "dirty snowballs".

FORCED PRECESSION OF THE COMETARY NUCLEUS WITH RANDOMLY PLACED ACTIVE REGIONS; Slawomira Szutowicz, Space Research Centre, Bartycka 18, 00-716 Warszawa, Poland

A cometary nucleus is modelled as a rotating, triaxial and axisymmetric ellipsoid that is forced to precess due to jets of ejected material. Precession of the nucleus is followed numerically using Euler's equations. Randomly placed regions of exposed ice on the surface of the nucleus are assumed to produce gas and dust. The solution of the heat conduction equation for each active region is used to find the gas sublimation rate, the jet acceleration and the torque. The effect of distribution of active regions across the nucleus surface, of the shape of cometary nucleus and of its spin period on the total gas production curve and on the precession of the spin axis during the orbital motion of the comet is discussed.

VELOCITY DISTRIBUTION OF FRAGMENTS OF CATASTROPHIC IMPACTS AND ORIGIN OF ASTEROID FAMILIES; Yasuhiko Takagi, Toho Gakuen Junior College, 3–11 Heiwagaoka, Meito-ku, Nagoya 465, Japan; Manabu Kato, Department of Earth Sciences, Nagoya University, Chikusa-ku, Nagoya 464-01, Japan; Hitoshi Mizutani, Institute of Space and Astronautical Science, Yoshinodai 3–1–1, Sagamihara 229, Japan

Velocity distribution of fragments produced by catastrophic disruption of parent bodies significantly affect the asteroid family formation. Although the experimental approach to this problem was not sufficient due to some technical difficulties, our new series of impact experiments (1) determined three-dimensional velocities of some tens of fragments. In this paper we report some results of our new experiments on three-dimensional velocities of fragments and the implication to the origin of asteroid families.

Experiments were performed in the impact velocity range of 140 to 650 m/sec. Targets were basalt and pyrophyllite. Projectiles were aluminum. Motions of fragments were recorded by a high-speed camera with a stereographic device in 1500–3000 frames/sec. The initial position and three-dimensional velocity of each fragment were determined from the analysis of the films. Each recovered fragment was weighed and identified with the image on the film. The total mass of fragments of which velocities could be determined is 75 to 98 percent of the initial target mass.

The main results obtained by the experiments are:

[1] The velocity range of fragments except fine particles in jetting is rather narrow, at most within a factor of 3. The mass dependence of velocity suggested by Nakamura and Fujiwara (3) is not very evident.

[2] The nondimensional impact stress (2) is an appropriate scaling parameter to describe the overall fragment velocity as well as the antipodal velocity. This result shows that the energy partition to kinetic energy of basalt fragments is an order of magnitude larger than that of pyrophyllite fragments, because the normalizing velocity of basalt is four times larger than that of pyrophyllite.

These results suggest the fragment velocity is not simply controlled by the surface energy, but by the shock wave strength and target properties which may yield complicated consequence of the shock wave generation, expansion, and decay (2). The results also support the conclusion on asteroid families that family members are single fragments, rather than rubble pile remnants (4).

REFERENCES: (1) Takagi, Y., M. Kato, and H. Mizutani (1991) *Lunar Planet. Sci. XXII*, 1371–1372 (2) Mizutani, H., Y. Takagi, and S. Kawakami (1990) *Icarus*, **87**, 307–326; (3) Nakamura, A. and A. Fujiwara (1990) Velocity distribution of fragments formed in simulated collisional disruption, submitted to *Icarus*; (4) Takagi, Y. and H. Mizutani (1990) *Asteroids, Comets, Meteors III*, 191–194

The Vicinity of Jupiter: A Region to Look for Comets

G. Tancredi [1,2] **and M. Lindgren** [1]
[1] *Astronomiska Observatoriet, Box 515, S-75120 Uppsala, Sweden*
[2] *Dept. Astronomía, Fac. de Ciencias, Montevideo, Uruguay*

Low-relative velocity and long-lasting encounters can dramatically change the orbital elements of a comet; the object could be temporarily bound to Jupiter for a period of several years.

It is well stated that most of the discoveries of comets ocurred just after a close encounter with the planet and a decrease of the perihelion distance of the comet.

So, why don't we look for comets during its close encounters with Jupiter rather than wait to find it afterwards ?

To estimate the feasibility of this proposal we have made dynamical computations and observational analysis of the Jupiter family of comets. We estimated the number of comets we should expect to find by integrating all observed Jupiter family comets and recording the time spent captured by the planet. The resultant numbers can increase if we consider that the Jupiter family population is far from being complete.

A criterion to distinguish the captured comets from other moving objects in the field is discussed.

A survey of comets during its close encounters with Jupiter could have important consequences in several aspects dealing with the dynamical evolution of minor bodies of the Solar System; e.g. :

* the origin of comets and the effects of encounters with Jupiter in the transfer of comets from the outer to the inner region of the Solar System
* the captured-hypothesis for the origin of the outer satellites of the outer planets.